

Preparation and Characterization of Ionic Liquid-based Electrodes for High Temperature Fuel Cells Using Cyclic Voltammetry

Sung-Kwan Ryu^{†,††}, Young-Woo Choi^{†,*}, Chang-Soo Kim[†], Tae-Hyun Yang[†],
Han-sung Kim^{††}, and Jin-Soo Park^{†††,*}

[†]*Hydrogen and Fuel Cell Research Department, Korea Institute of Energy Research (KIER),
71-2, Jang-dong, Yuseong-gu, Daejeon 305-343, Republic of Korea*

^{††}*Department of Chemical Engineering, Yonsei University, 134 Sinchon-dong,
Seodaemun-gu, Seoul 120-749, Republic of Korea*

^{†††}*Department of Environmental Engineering, College of Engineering, Sangmyung University,
300 Anseo-dong, Dongnam-gu, Cheonan, Chungnam Province 330-720, Republic of Korea*

(Received January 21, 2013 : Accepted February 25, 2013)

Abstract: In this study, a catalyst slurry was prepared with a Pt/C catalyst, Nafion ionomer solution as a binder, an ionic liquid (IL) (1-butyl-3-methylimidazolium tetrafluoroborate), deionized water and ethanol as a solvent for the application to polymer electrolyte fuel cells (PEFCs) at high-temperatures. The effect of the IL in the electrode of each design was investigated by performing a cyclic voltammetry (CV) measurement. Electrodes with different IL distributions inside and on the surface of the catalyst electrode were examined. During the CV test, the electrochemical surface area (ESA) obtained for the Pt/C electrode without ILs gradually decreased owing to three mechanisms: Pt dissolution/redeposition, carbon corrosion, and place exchange. As the IL content increased in the electrode, an ESA decrement was observed because ILs leaked from the Nafion polymer in the electrode. In addition, the CVs under conditions simulating leakage of ILs from the electrode and electrolyte were evaluated. When the ILs leaked from the electrode, minor significant changes in the CV were observed. On the other hand, when the leakage of ILs originated from the electrolyte, the CVs showed different features. It was also observed that the ESA decreased significantly. Thus, leakage of ILs from the polymer electrolyte caused a performance loss for the PEFCs by reducing the ESA. As a result, greater entrapment stability of ILs in the polymer matrix is needed to improve electrode performance.

Keywords : High temperature polymer electrolyte fuel cell, Ionic liquid, Electrode, Electrochemistry

1. Introduction

Polymer electrolyte fuel cells (PEFCs) are well studied for a variety of applications owing to their environmentally friendly nature, efficiency, and high power density. Recently, PEFC technology has led to a demand for the operation of PEFCs at high temperatures for higher efficiency, enhanced CO tolerance, and easy water management.¹⁻⁴⁾ However, there are serious problems with the operation of

PEFCs at high temperatures. The commercial perfluorosulfonic polymers such as NafionTM are dependent on the presence of water to solvate the protons from the sulfonic acid groups. To solve this problem, some alternative approaches have been proposed. Recently, non-aqueous proton-conducting membranes based on poly (vinylidene fluoride-hexafluoropropylene) (PVdF-HFP),^{5,6)} Nafion,⁷⁾ poly (acrylonitrile) (PAN), poly (ethyleneoxide) (PEO), poly (vinylalcohol) (PVA)⁸⁾ and sulfonated poly (ether ether ketone) (SPEEK)⁹⁾ have been prepared by the impregnation of a variety of room temperature ionic liquids (RTILs). Thus, ionic liquids (ILs) have been

*E-mail: cozmoz67@kier.re.kr
energy@smu.ac.kr

considered as good candidates for the substituent of water in sulfonated polymers for high-temperature PEFCs owing to their intrinsic properties such as good electrochemical stability, high ionic conductivity, and non-flammability.¹⁰⁻¹³⁾ For the application of ILs in PEFCs, IL-based composite membranes must be developed. Cho et al.¹⁴⁾ reported that ILs in the composite membranes behaved like water under non-aqueous conditions. The trend in ionic conductivity of the composite membranes depends on the content of the ILs and the degree of sulfonation (DS) of the polymer matrix. Thus, composite membranes with higher amounts of ILs and more degrees of sulfonation (DS) of the polymer matrix showed higher ionic conductivity. Specifically, the ionic conductivity of one composite membrane (Nafion:IL ratio (wt%) = 33.3:66.7) was 0.05 S/cm at 180°C.

In general, PEFC electrodes contain a Nafion ionomer, an electrocatalyst, usually a platinum electrocatalyst supported on carbon, and sometimes polytetrafluoroethylene (PTFE). In particular, the Nafion ionomer helps to increase a three-phase boundary reaction zone of catalytic activity and catalyst utilization, and the electrocatalyst plays a binding role to form electrodes for the fuel cell.¹⁵⁾ Furthermore, by helping to retain moisture, it protects the electrodes from membrane dehydration. As previously mentioned, sulfonated polymers exhibit poor proton conductivity at high temperatures because of the evaporation of water in the polymer. It is important to improve the performance of IL-based electrodes. However, sulfonated polymers containing ILs have a serious problem, which is the leakage of the IL from the polymer due to poor entrapment stability of the ILs within the polymer matrix.¹⁴⁾ In

the latter case, leaked ILs will affect the platinum catalyst surface of the membrane electrode assembly (MEA), resulting in performance loss of the PEFC.

In the present work, the catalyst slurry was prepared with various amounts of ionic liquids. The effects of ILs on the electrochemical properties of the electrode were investigated by performing cyclic voltammetry (CV) measurements for the various electrodes with different amounts of ILs in a strong supporting electrolyte. In addition, cyclic voltammograms under two simulated environments, *i.e.*, IL leakages from the Nafion ionomer in the electrode and from the polymer electrolyte, were investigated.

2. Experimental

2.1. Catalyst slurry preparation

The electrocatalyst used for the preparation of the electrode was 40 wt% Pt/C from Johnson Matthey. A 5 wt% Nafion solution supplied by Dupont, Inc., USA, was used as the binder in the electrode. For the preparation of the catalyst slurry, the required quantity of 40 wt% Pt/C was placed in a beaker, and a few drops of water were added. The required quantities of 5 wt% Nafion solution, ethanol, and the IL (1-butyl-3-methylimidazolium tetrafluoroborate) were added and ultrasonically dispersed for 30 min. Then, the catalyst slurry was mixed by a magnetic stirrer for 24 h. As listed in Table 1, three types of experiments were designed to produce the cyclic voltammograms of various electrodes.

2.2. Electrochemical evaluation

The electrochemical measurement was performed in a conventional three-electrode electrochemical cell

Table 1. Three types of experiments designed to generate cyclic voltammograms with various electrodes

Experiment Type	Real environment	Intended environment	Electrode	Nafion:IL ratio (wt%)
Exp. I	Electrode containing IL	Leakage of IL from Nafion ionomer as a binder in electrode	Electrode a	100:0
			Electrode b	50:50
			Electrode c	55.6:44.4
			Electrode d	66.7:33.3
			Electrode e	77:23
Exp. II	Injection of IL into H ₂ SO ₄	Leakage of IL from polymer electrolyte	Electrode f	0:100
			Electrode g	0:500
Exp. III	Reference electrode	-	Electrode h	100:0

using $\text{Hg}/\text{Hg}_2\text{Cl}_2/\text{Cl}^-$ as a reference electrode (0.241 V vs. the normal hydrogen electrode (NHE)) and a platinum wire as a counter electrode. The working electrodes were prepared just before the electrochemical measurement. A glassy carbon (GC) electrode with an area of 0.04 cm^2 was employed as the working electrode. On the clean GC surface, $5 \mu\text{L}$ of catalyst slurry was added, measured with a digital pipette. Then, the working electrode was dried at room temperature. A glass cell that was filled with $0.5 \text{ M H}_2\text{SO}_4$ as a supporting electrolyte was used for electrochemical measurements. Electrochemical measurements were performed using a potentiostat (Solartron Analytical, Model 1470E). During CV, argon gas was continuously bubbled through the supporting electrolyte to eliminate the dissolved oxygen. Electrochemical measurements were performed using three types of experiments, as listed in Table 1. Fig. 1 shows the schematic of each experiment. Experiment III was measured with only a Pt/C electrode as the reference electrode. Experiments I and II were the simulated conditions of the leaked ILs from the electrode and polymer electrolyte, respectively. In Experiments I and III, before the collection of electrocatalytic activities of the electrode, potential pulses between 0 and 1.2 V (NHE) were applied to stabilize the morphology and surface state of the electrode. Then, during 100 cycles, cyclic voltammograms were produced at a sweep rate of 20 mVs^{-1} and 0-1.2 V (NHE) of potential range. In the case of Experiment II, first the electrode was applied with the same potential to stabilize the electrode surface. Then, cyclic voltammograms were produced at a sweep rate of 20 mVs^{-1} for one cycle. After one cycle of CV, the specified amount of the

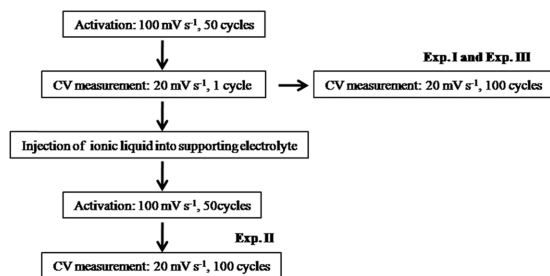


Fig. 1. Scheme of three types of cyclic voltammetry procedures.

IL was injected into the supporting electrolyte, and the surface stabilizing process was performed again. Finally, cyclic voltammograms were produced at a sweep rate of 20 mVs^{-1} during 100 cycles.

3. Results and Discussion

3.1. Electrochemical characteristics of the electrodes by CV

CV is typically used to characterize the fuel cell catalyst activity in more detail. In a standard CV measurement, the potential of a system is swept back and forth between two voltage limits while the current response is measured. The voltage sweep is generally linear with time, and the plot of the resulting current against voltage is called a cyclic voltammogram. An illustration of a typical CV waveform is shown in Fig. 2.¹⁶⁾

In fuel cells, the CV measurement is performed by sweeping the system voltage between approximately

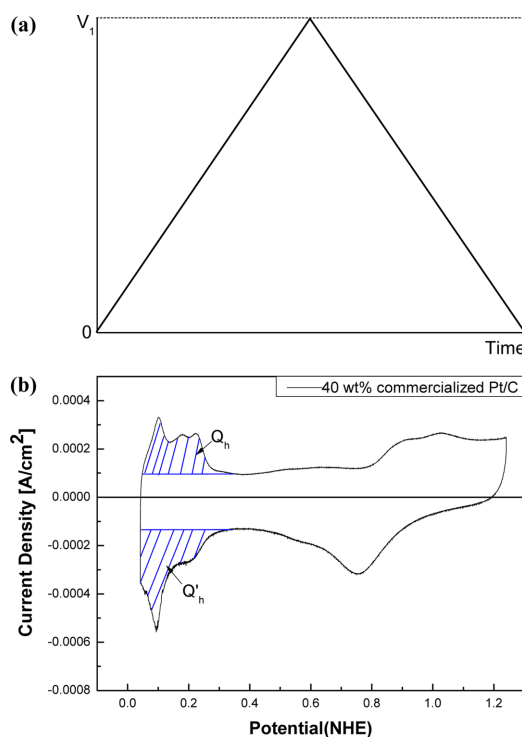


Fig. 2. (a) Schematic plots of a CV waveform and (b) a fuel cell catalyst CV curve (The peaks marked Q_h and Q'_h represent the hydrogen adsorption and desorption peaks on the platinum fuel cell catalyst surface).

0 V and 1 V with respect to the anode. An example of a cyclic voltammogram from a fuel cell is shown in Fig. 2. When the potential increases from 0 V, a current begins to flow. There are two contributions to this current. One contribution is a capacitive charging current that flows in response to the linearly changing voltage. The second current response is nonlinear and corresponds to a hydrogen adsorption reaction occurring on the electrochemically active cathode catalyst surface. As the voltage increases further, this reaction current reaches a peak and then falls off as the entire catalyst surface becomes fully saturated with hydrogen. In general, the cyclic voltammogram of a platinum catalyst has three regions, which are electrochemical adsorption/desorption of hydrogen (0-0.4 V vs. NHE), double layer charging (0.4-0.6 V vs. NHE), and PtOH formation/reduction (0.6-1.2 V vs. NHE).

It is also believed that the electrochemical surface area (ESA) is one of the important parameters for characterizing a fuel cell electrode. A large ESA implies a better electrode, as more catalyst sites are available for electrochemical reaction in the electrode.

As shown in Fig. 2, the ESA is determined by the total charge (Q_h) attributed to hydrogen adsorption/desorption according to the following equation:¹⁷⁾

$$ESA = \frac{Q_h}{0.21} \quad (1)$$

where Q_h (mC) corresponds to the area under the hydrogen adsorption reaction peak (0.05-0.4 V vs. NHE) in the cyclic voltammogram. The electrical charge associated with the monolayer adsorption of hydrogen on a Pt catalyst is 0.21 (mC/cm²).

Repeated potentiodynamic cycling between hydrogen adsorption and the oxide formation potential, as well as electrochemical treatment as in constant potential holds, can change the ESAs of catalyst electrodes. The effect of cycling repeatedly between 0-1.2 V (NHE) on the cyclic voltammogram of a Pt catalyst electrode is shown in Fig. 3. The degradation in ESAs can be ascribed to several mechanisms such as an increase in particle size of the Pt particles due to dissolution/redeposition/surface migration, carbon corrosion and the consequent loss of Pt dispersion, and change in the structure and composition of platinum by place-exchange processes.

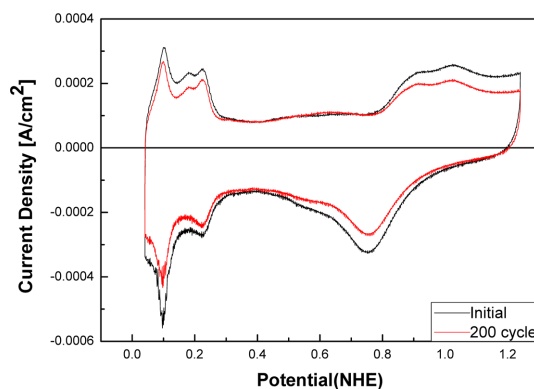


Fig. 3. CV of commercialized MEA after repeating CV test (40 wt% commercialized Pt/C electrode, scan rate 20 mV s⁻¹).

Dissolution of Pt from small catalyst particles followed by its redeposition on a larger particle can cause an increase in particle size and thus a decrease in the ESA of Pt.¹⁸⁾ However, if Pt dissolves without redeposition in the electrolyte, it will decrease the particle size, increase the surface roughness, and thus increase ESA. Kinoshita et al.¹⁹⁾ studied the effect of potential cycling on Pt dissolution for a Pt foil sheet and for a graphite-supported Pt electrode, with the amount of dissolved Pt differing by two orders of magnitude. The ESA increased for the foil in spite of the high rate of Pt dissolution, whereas the area decreased for the other two electrodes. If the dissolved platinum were to redeposit on a large particle, assisted by electrochemical reduction and surface diffusion, then the particle size can increase leading to a reduction in the ESA. Pt dissolution and redeposition are likely to occur in the potential region of 1.0-1.2 V (NHE), as suggested by the potential-PH diagram for a Pt catalyst.²⁰⁾

Corrosion of carbon support can lead to movement and the consequent agglomeration of Pt particles. Carbon oxidation occurs through two pathways: an incomplete oxidation leading to the formation of surface groups or a complete oxidation to gaseous carbon dioxide. In cycling at potentials below 1 V, carbon corrosion is influenced by the presence of Pt. At these potentials, Pt interacts with water to form adsorbed oxygen species such as Pt-OH_{ads}, the stability of which depends strongly on the applied potential.²¹⁾ Carbon oxidation to gaseous species can

cause agglomeration of Pt particles leading to a decrease in surface area due to the loss of catalyst dispersion.^{22,23)}

3.2. Place-exchange mechanism

When Pt interacts with a chemisorbed OH species, a place exchange of OH species can occur leading to changes in the chemical composition of the Pt catalyst.²⁴⁻²⁷⁾ Pt-OH place-exchange reactions can occur during cycling when the Pt surface undergoes repetitive formation and reduction of electrochemisorbed OH. Chemisorbed hydrogen can also alter the surface reconstruction and cause an increase in surface stress in the Pt catalyst. The surface oxygen can react with water to generate a hydroxide radical, or it can undergo place exchange. The surface hydroxyl species can also undergo place exchange with Pt atoms. This modified Pt may have a different interaction with oxygen and hydrogen.

3.3. Changes in the ESAs with CV cycling

Fig. 4 shows the CVs obtained for a Pt/C electrode without an IL in the potential range of 0-1.2 V (NHE). Some typical peaks are observed showing the oxidation-reduction of Pt and the desorption-adsorption of hydrogen on the Pt surface. Changes in the ESA for 100 cycles of CV are also observed. As shown in Fig. 4, the ESA gradually decreased during repeated cycles. After 100 cycles of CV, the ESA decreased about 13% with respect to the initial ESA. As mentioned above, the ESA

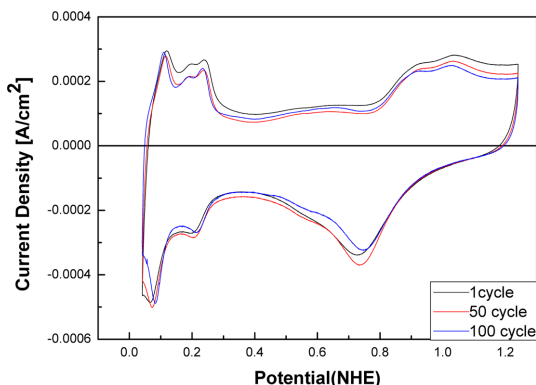


Fig. 4. CVs of an electrode without an ionic liquid at different CV cycles (40 wt% Pt/C electrode, scan rate 20 mV s⁻¹).

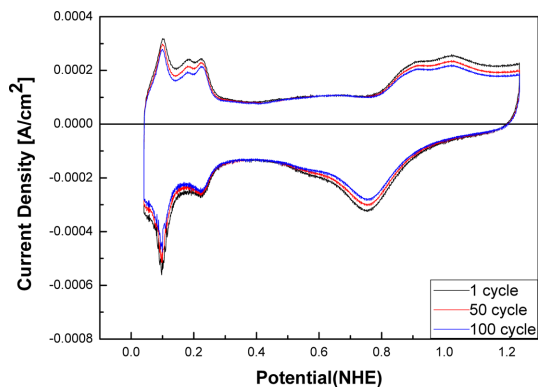


Fig. 5. CVs of an electrode containing an IL at different CV cycles (40 wt% Pt/C electrode containing the IL, scan rate 20 mV s⁻¹).

decrement of Pt catalysts can be explained by Pt dissolution/redeposition, carbon corrosion, and Pt-exchange during the CV measurements.²⁸⁻³⁰⁾ For comparison, the CVs of a Pt/C electrode containing an IL are shown in Fig. 5. It can be observed that the CVs of Fig. 5 are similar to those of Fig. 4 in both shape and the decreasing tendency of ESA. It was predicted that the addition of the ILs in the electrode would have less influence on the CV measurements. However, as shown in Fig. 6, the ESA obtained for the Pt/C electrode containing an IL decreased even more. This can be explained by partial coverage of the Pt surface and electrode pore caused by leaked ILs from the Nafion polymer in the electrode as well as by three mechanisms: Pt dissolution/redeposition, carbon corrosion, and Pt-

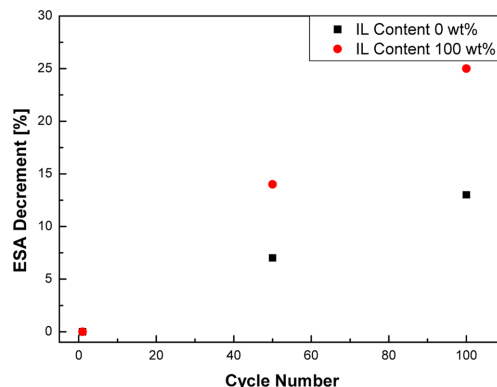


Fig. 6. Changes in ESA decrement by the number of cycle obtained from an electrode with different IL contents.

exchange. Fig. 6 shows that the rate of decrease in ESA for the Pt/C electrode containing an IL was higher than the rate of decrease in ESA for the Pt/C electrode without an IL during CV cycling. Thus, as the cycle number increases, more IL may be leaked from the electrode so that the ESA loss of the Pt/C electrode containing an IL is greater.

Many researchers have investigated the effect of the Nafion ionomer distribution in the catalyst layer on cell performance and improved electrode performance.³¹⁻³³ It was also reported that optimum Nafion loading exists for good performance in fuel cells.³⁴⁻³⁶ Passalacqua et al.³⁷ studied the effect of various Nafion amounts in the electrode. They reported that the effective area for the fuel cell reactions could be smaller owing to coverage of the active Pt surface and electrode pore for low or high Nafion loading in the electrode. According to the IL content in the electrode, it was expected that

different volumes of IL would leak from the Nafion polymer. In order to clarify this expectation, the CVs of Pt/C electrodes with various amounts of the IL were observed to investigate the effect of leaked IL from the electrode. Fig. 7(a) shows the CVs obtained for Pt/C electrodes with different IL contents. Typical hydrogen adsorption and desorption peaks similar to those shown in Fig. 4 and Fig. 5 were observed. However, as the IL content increased in the electrode, decreasing ESA was observed as shown in Fig. 7(a). Thus, when the IL content in the electrode is high, more of the IL might be leaked from the Nafion polymer in the electrode. As a result, smaller ESA decrements were observed with respect to the Pt/C electrode without an IL, as shown in Fig. 7(b).

Cho et al.¹⁴ investigated composite membranes with various ILs and IL contents. They found that the ability to entrap the IL in the Nafion matrix is poorer than in other sulfonated poly(aryl ether ketone) (SPAEEK-6F) matrices. They also reported that the polymer matrix influences the performance of the composite membrane. The IL in Nafion-based composite membranes was easily leaching-out, which means that it is not suitable for use in actual device applications despite having relatively high conductivity. Thus, the polymer matrix also plays an important role in the immobilization property of ILs in composite membranes.

Oono et al.³⁸ studied the influence of the phosphoric acid-doping level in a polybenzimidazole (PBI) membrane on fuel cell performance. They prepared PBI membranes with acid-doping levels of 65%, 71%, 75%, and 78%. They found that there was insufficient phosphoric acid migrating from the PBI membrane to the catalyst layers to obtain a sufficient active area for a single cell with a doping level below 75%. They also reported that the catalyst layer was flooded with phosphoric acid that migrated from the PBI membrane for a single cell with a doping level above 75%. Thus, we needed to investigate the effect of leaked ILs from polymer electrolytes on Pt electrodes.

In order to clarify the influence of the leaked IL from the polymer electrolyte, the CVs of two simulated conditions were investigated. Fig. 8(a) shows the CVs obtained for a Pt/C electrode without

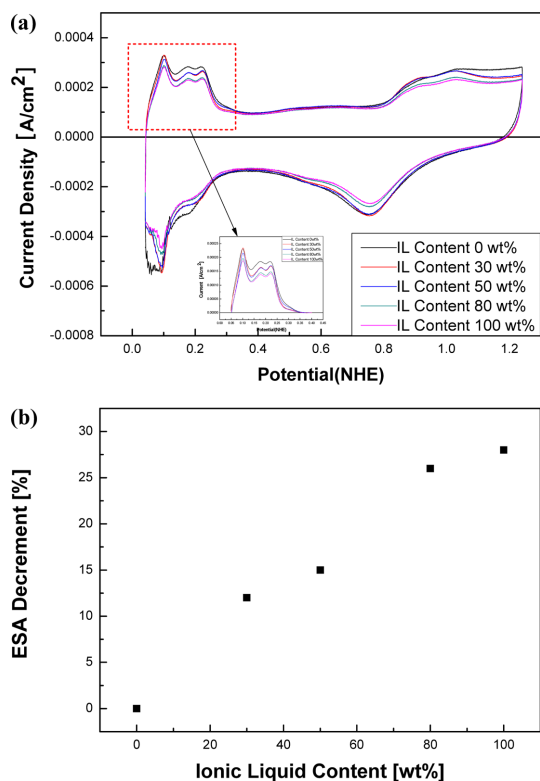


Fig. 7. (a) CVs of an electrode containing various IL contents in the electrode and (b) the decrement of ESA with the content of IL in the electrode.

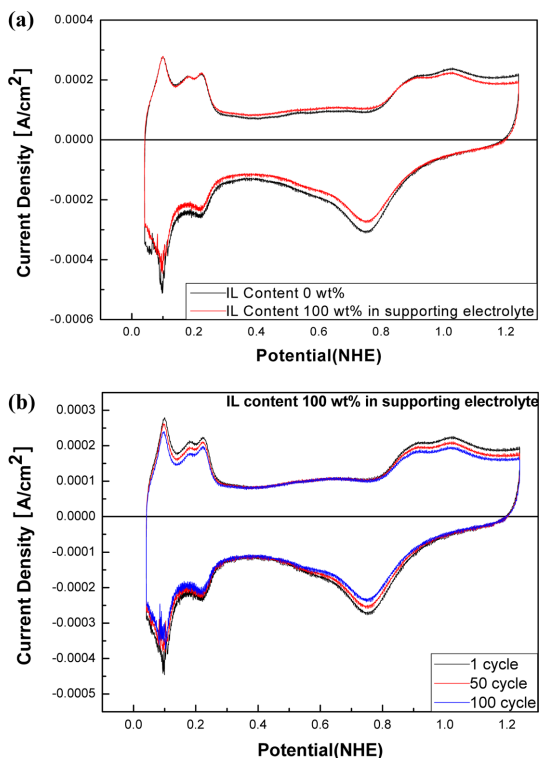


Fig. 8. CVs of an electrode (a) with a small amount of IL injected into the supporting electrolyte (scan rate 20 mV s^{-1} , 100 cycles) and (b) with the number of cycle.

an IL compared to the CVs obtained for a Pt/C electrode with a small amount of IL (the maximum volume of IL leaked from the electrode) injected into the supporting electrolyte. Fig. 8(a) shows the two peaks corresponding to the oxidation-reduction of Pt and the adsorption-desorption of hydrogen on the Pt surface. It was also observed that the ESA decrement rate was similar to that in Fig. 5. Thus, when a small volume of an IL is injected into the supporting electrolyte, it appears that the effect on ESA decrement is not serious.

On the other hand, the CVs obtained for a Pt/C electrode with a large volume of IL (the maximum possible amount of IL leaked from the polymer electrolyte) injected into the supporting electrolyte is shown in Fig. 9(a). The CV curves showed different features compared to the CV obtained for the Pt/C electrode without an IL. The CVs for the large volume of IL had no distinguishable peaks for hydrogen desorption-adsorption on the Pt surface, and

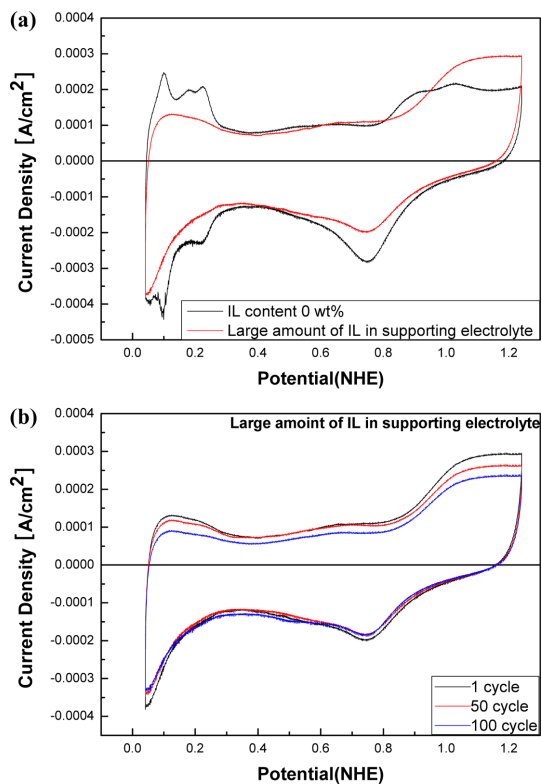


Fig. 9. CVs of an electrode (a) with a large volume of IL injected into the supporting electrolyte (scan rate 20 mV s^{-1} , 100 cycles) and (b) with the number of cycle.

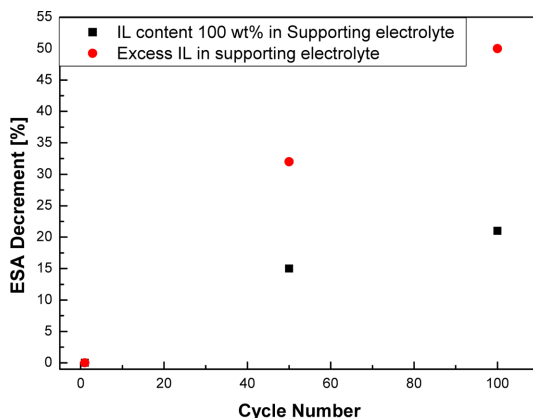


Fig. 10. Variation of ESA decrement during the CV cycles obtained from the electrode in the supporting electrolyte with different IL contents.

the ESA decreased significantly, as shown in Fig. 9(b). As shown in Fig. 10, large amounts of IL leakage from the polymer electrolyte showed about a

two times higher ESA decrement rate and worse results in electrochemical properties of the electrodes. It appears that when a large volume of IL leaked from the polymer electrolyte, the Pt surface and electrode pore were filled with the leaked IL.

4. Conclusion

For non-humidified and high-temperature PEFCs, ILs are used to replace water in the Nafion polymer. ILs generally show good electrochemical stability, high ionic conductivity, and non-flammability. However, when sulfonated polymers contain ILs, the ILs are easily leached out of the polymer matrix by the pairing relation reported elsewhere.¹⁴⁾ The present study has investigated the effect of ILs on the electrochemical properties of Pt/C electrodes with various IL contents using CV. The cyclic voltammograms obtained for each electrode showed the typical peaks of hydrogen adsorption and desorption except for one experiment (leaked ILs from a polymer electrolyte as a simulated condition). As the IL content of the Pt/C electrode and the cycling number increased, the ESA decreased owing to the coverage of the Pt surface and electrode pores caused by leaked IL from the Nafion polymer as well as three mechanisms: Pt dissolution/redeposition, carbon corrosion, and place exchange. After repeated cycles, the CVs obtained for the Pt/C electrode containing an IL showed an ESA decrement rate two times higher than that showed for the CVs obtained for the Pt/C electrode without an IL.

It could be that ILs leaked out from the IL composite membrane as well as from the Nafion polymer in the electrode. In order to clarify the effect of a leaked IL from a polymer electrolyte, CVs were produced with the injection of ILs into the supporting electrolyte. When a small amount of an IL was injected into the supporting electrolyte, the CVs showed typical hydrogen adsorption and desorption peaks. The ESA decrement rate also showed a similar tendency to the ESA decrement rate of an IL-containing electrode. However, when a large volume of an IL was injected into the supporting electrolyte, the ESA decreased more rapidly owing to the effect of the added ILs. It appears that a large amount of ILs filled the active

site and pores of the electrode. Thus, a large amount of a leaked IL from the polymer electrolyte had a negative influence on the decrement of ESA. Finally, the entrapment stability of the ILs by the polymer matrix was important to improve the Pt/C electrode containing ILs. Thus, it is important to make the electrode and polymer electrolyte in which ILs are embedded with Nafion polymer as stable as possible.

Acknowledgements

This work was supported in part by the project, 20113020030040, of the Korea Institute of Energy Technology Evaluation and Planning (KETEP) grant and in part by the World Premier Materials (WPM) (No. 10037748) of the Korea Evaluation Institute of Industrial Technology (KEIT) grant funded by the Ministry of Knowledge Economy, Republic of Korea.

References

1. J. Zhang, Z. Xie, J. Zhang, Y. Tang, C. Song, T. Navessin, Z. Shi, D. Song, H. Wang, D. P. Wilkinson, Z. S. Liu, and S. Holdcroft, 'High temperature PEM fuel cells', *J. Power Sources*, **160**, 872 (2006).
2. W. H. J. Hogarth, J. C. Diniz da Costa, and G. Q. (Max) Lu, 'Solid acid membranes for high temperature (>140°C) proton exchange membrane fuel cells', *J. Power. Sources*, **142**, 223 (2005).
3. J. Hu, H. Zhang, Y. Zhai, G. Liu, J. Hu, and B. Yi, 'Performance degradation studies on PBI/H3PO4 high temperature PEMFC and one-dimensional numerical analysis', *Electrochim. Acta*, **52**, 394 (2006).
4. A. S. Aričo, A. Stassi, E. Modica, R. Ornelas, I. Gatto, E. Passalacqua, and V. Antonucci, 'Performance and degradation of high temperature polymer electrolyte fuel cell catalysts', *J. Power. Sources*, **178**, 525 (2008).
5. J. Fuller, A. C. Breda, and R. T. Carlin, 'Ionic Liquid-Polymer Gel Electrolytes', *J. Electrochem. Soc.*, **144**, L67 (1997).
6. Z. Zhou, S. Li, Y. Zhang, M. Liu, and W. Li, 'Promotion of Proton Conduction in Polymer Electrolyte Membranes by 1H-1,2,3-Triazole', *J. Am. Chem. Soc.*, **127**, 10824 (2005).
7. A. Schechter and R. F. Savinell, 'Imidazole and 1-methyl imidazole in phosphoric acid doped polybenzimidazole, electrolyte for fuel cells', *Solid State Ionics*, **147**, 181 (2002).
8. J. Sun, L. R. Jordan, M. Forsyth, and D. R. MacFarlane, 'Acid-Organic base swollen polymer membranes', *Electrochim. Acta*, **46**, 1703 (2001).
9. K. D. Kreuer, A. Fuchs, M. Ise, M. Spaeth, and J. Maier,

- 'Imidazole and Pyrazole-base proton conducting polymers and liquids', *Electrochim. Acta*, **43**, 1281 (1998).
10. B. Singh and S. S. Sekhon, 'Ion conducting behaviour of polymer electrolytes containing ionic liquids' *Chem. Phys. Lett.*, **34**, **414**, (2005).
 11. M. Doyle, S.K. Choi, and G. Proulx, 'High-Temperature Proton Conducting Membranes Based on Perfluorinated Ionomer Membrane-Ionic Liquid Composites', *J. Electrochem. Soc.*, **147**, 34 (2000).
 12. A. Lewandowski and A. Swinderski, 'New composite solid electrolytes based on a polymer and ionic liquids', *Solid State Ionics*, **169**, 21 (2004).
 13. Q. Che, B. Sun, and R. He, 'Preparation and characterization of new anhydrous, conducting membranes based on composites of ionic liquid trifluoroacetic propylamine and polymers of sulfonated poly (ether ether) ketone or polyvinylidene fluoride' *Electrochim. Acta*, **53**, 4428 (2008).
 14. E. K. Cho, J. S. Park, S. S. Sekhon, G. G. Park, T. H. Yang, W. Y. Lee, C. S. Kim, and S. B. Park, 'A Study on Proton Conductivity of Composite Membranes with Various Ionic Liquids for High-Temperature Anhydrous Fuel Cells', *J. Electrochem. Soc.*, **156** (2), B197 (2009).
 15. G. Sasikumar, J. W. Ihm, and H. Ryu, 'Dependence of optimum Nafion content in catalyst layer on platinum loading', *J. Power Sources*, **132**, 11 (2004).
 16. R. O'Hayre, S. W. Cha, W. Colella, and F. B. Prinz, *Fuel Cell Fundamentals 2nd Ed.*, Wiley, p. 252 (2006).
 17. Y. Y. Shao, G. P. Yin, and Y. Z. Gao, Chin. 'Electrochemical surface area enhanced by dimethyl ether (DME) electrooxidation', *J. Inorg. Chem.*, **21**, 1060 (2005).
 18. R. M. Darling and J. P. Meyers, 'Kinetic Model of Platinum Dissolution in PEMFCs', *J. Electrochem. Soc.*, **150**, A1523 (2003).
 19. K. Kinoshita, J. T. Lundquist, and P. Stonehart, 'Potential cycling effects on platinum electrocatalyst surfaces', *J. Electroanal. Chem. Interfacial Electrochem.*, **48**, 157 (1973).
 20. J. F. Liopis and F. Colom, *In Encyclopedia of Electrochemistry of Elements, Vol. VI*, (Ed: A. J. Bard), Marcel Dekker, New York, p. 169 (1976).
 21. R. Rajagopalan, A. Ponnaiyan, P. J. Mankidy, A. W. Brooks, B. Yi, and H. C. Foley, 'Molecular sieving platinum nanoparticle catalysts kinetically frozen in nanoporous carbon', *Chem. Commun. (Cambridge)*, **21**, 2498 (2004).
 22. F. Rodriguez-Reinoso, 'The role of carbon materials in heterogeneous catalysis', *Carbon*, **36**, 159 (1998).
 23. F. Coloma, A. Sepulvedaescibano, J. L. G. Fierro, and F. Rodriguez-Reinoso, 'Preparation of Platinum Supported on Pregraphitized Carbon Blacks' *Langmuir*, **10**, 750 (1994).
 24. W. Z. Li, C. H. Liang, W. J. Zhou, J. S. Qiu, Z. H. Zhou, G. Q. Sun, and Q. Xin, 'Preparation and Characterization of Multiwalled Carbon Nanotube-Supported Platinum for Cathode Catalysts of Direct Methanol Fuel Cells', *J. Phys. Chem. B*, **107**, 6292 (2003).
 25. M. L. Toebes, F. F. Prinsloo, J. H. Bitter, A. J. van Dillen, and K. P. de Jong, 'Influence of oxygen-containing surface groups on the activity and selectivity of carbon nanofiber-supported ruthenium catalysts in the hydrogenation of cinnamaldehyde', *J. Catal.*, **214**, 78 (2003).
 26. J. L. Figueiredo, M. F. R. Pereira M. M. A. Freitas, and J. J. M. Orfao, 'Modification of the surface chemistry of activated carbons', *Carbon*, **37**, 1379 (1999).
 27. Z. Siroma, N. Fujiwara, T. Ioroi, S. Yamazaki, K. Yasuda, and Y. Miyazaki, 'Dissolution of Nafion® membrane and recast Nafion® film in mixtures of methanol and water', *J. Power Sources*, **126**, 41 (2004).
 28. C. H. Paik, T. D. Jarvi, and W. E. O'Grady, 'Extent of PEMFC Cathode Surface Oxidation by Oxygen and Water Measured by CV', *Electrochem. Solid-State Lett.*, **7**, A82 (2004).
 29. M. S. Wilson, F. H. Garzon, K. E. Sickafus, and S. Gottesfeld, 'Surface area loss of supported platinum in polymer electrolyte fuel cells', *J. Electrochem. Soc.*, **140**, 2872 (1993).
 30. R. M. Darling and J. P. Meyers, 'Kinetic Model of Platinum Dissolution in PEMFCs', *J. Electrochem. Soc.*, **150**, A1523 (2003).
 31. D. Lee and S. Hwang, 'Effect of loading and distributions of Nafion ionomer in the catalyst layer for PEMFCs', *International Journal of Hydrogen Energy*, **33**, 2790 (2008).
 32. E. Passalacqua, F. Lufitano, G. Squadrio, A. Patti, and L. Giorgi, 'Nafion content in the catalyst layer of polymer electrolyte fuel cells: effects on structure and performance', *Electrochim. Acta*, **46**, 799 (2001).
 33. J. Sasikumar, J. W. Ihm, and H. Ryu, 'Dependence of optimum Nafion content in catalyst layer on platinum loading', *J. Power Sources*, **132**, 11 (2004).
 34. E. Antolini, L. Giorgi, A. Pozio, and E. Passalacqua, 'Influence of Nafion loading in the catalyst layer of gas-diffusion electrodes for PEFC', *J. Power Sources*, **77**, 136 (1999).
 35. S. Gamburgzev and A. Appleby, 'Recent progress in performance improvement of the proton exchange membrane fuel cell (PEMFC)', *J. Power Sources*, **107**, 5 (2002).
 36. Z. Qi and A. Kaufman, 'Low Pt loading high performance cathodes for PEM fuel cells', *J. Power Sources*, **113**, 37 (2003).
 37. E. Passalacqua, F. Lufitano, G. Squadrito, A. Patti, and L. Giorgi, 'Nafion content in the catalyst layer of polymer electrolyte fuel cells: effects on structure and performance', *Electrochim. Acta*, **46**, 799 (2001).
 38. Y. Oono, A. Sounai, and Michio Hori, 'Influence of the phosphoric acid-doping level in a polybenzimidazole membrane on the cell performance of high-temperature proton exchange membrane fuel cells', *J. Power Sources*, **189**, 943 (2009).